Available online at www.sciencedirect.com
ScienceDirect
Carbohydrate Polymers 68 (2007) 173–186
Carbohydrate Polymers
www.elsevier.com/locate/carbpol

The role played by the interactions of small molecules with chitosan and their transition temperatures. Glass-forming liquids: 1,2,3-Propantriol (glycerol)

I. Quijada-Garrido [a,*], V. Iglesias-González [a], J.M. Mazón-Arechederra [b], J.M. Barrales-Rienda [a]

[a] *Departamento de Química-Física de Polímeros, Instituto de Ciencia y Tecnología de Polímeros (ICTP), Consejo Superior de Investigaciones Científicas (CSIC), Juan de la Cierva 3, E-28006 Madrid, Spain*
[b] *Centro de Investigación, Compañía Española de Petróleos, S. A. (CEPSA), Polígono Industrial San Fernando II, Picos de Europa 7, E-28850 TORREJÓN DE ARDOZ, Madrid, Spain*

Received 19 May 2006; received in revised form 17 July 2006; accepted 24 July 2006
Available online 7 September 2006

Abstract

Dynamic behaviour of chitosan and chitosan blended with 1,2,3-propantriol (glycerol) has been studied by dynamic mechanical analysis (DMTA), solid-state NMR and differential scanning calorimetry (DSC). Two relaxation processes appear in pure chitosan, one at high temperature, the α-relaxation which has been attributed to its glass transition temperature and interpreted as torsional oscillations between two glucopyranose rings across a glucosidic oxygen and a cooperative hydrogen bonds reordering. And the other, a low temperature relaxation, β, which is associated with local motions of lateral groups, namely, $–NH_2$ or as $–NH^+{}_3{}^-OOC–CH_3$ (quitosonium acetate), $–CH_2OH$ and in some extension $–NH–OC–CH_3$, mainly. The incorporation of glycerol in the blends results, as detected by DMTA analysis, in a substantial depression of the glass transition of the chitosan matrix due to a plasticization process. The β-relaxation in the blends, which also depends on glycerol concentration, has been interpreted as motions of the side chains of chitosan linked to glycerol by hydrogen bonding. The interaction between both components was also investigated by solid-state NMR, which revealed a decreasing of the glycerol mobility with increasing chitosan content in the blends and an increase of chitosan mobility for enriched glycerol blends. The measurements of the proton spin-lattice relaxation time in the rotating frame, $T^{H}_{1\rho}$ for 50% mol chitosan blend revealed that the blend is homogeneous in a length scale of few nanometers. As the glycerol concentration is increased, two relaxation times could be distinguished, corresponding to glycerol and chitosan domains. For high concentration glycerol blends, we have assumed a "*clustering model*" for the glycerol molecules sorbed on chitosan macromolecular chains consisting of a two-step mechanism. A first step, in which the solvent is sorbed by means of hydrogen bonds on polymer-specific sites such as –OH and $–NH_2$ or as $–NH^+{}_3{}^-OOC–CH_3$ (quitosonium acetate), and a second one, a solvent clustering around the first sorbed solvent molecules forming a hydrogen bonded network of glycerol molecules.

Keywords: Chitosan; Glycerol; Blends; Thermal relaxations

1. Introduction

Chitosan [β-(1,4)-2-amino-2-deoxy-D-glucopyranose] is a natural polymer derived by deacetylation of chitin, which is the second most abundant biopolymer in nature after cellulose (Shahidi, Arachchi, & Jeon, 1999). Because chitosan has functional groups like hydroxyls, amines and amides, which can act as hydrogen bond acceptors or donors, it can be probably bonded or linked with hydrogen bond donors or acceptor compounds. The properties of chitosans are very much dependent on the degree of deacetylation (DAD), which depends on the synthesis of

* Corresponding author. Tel.: +34 91 562 29 00; fax: +34 91 5644853.
E-mail address: iquijada@ictp.csic.es (I. Quijada-Garrido).

0144-8617/$ - see front matter © 2006 Elsevier Ltd. All rights reserved.
doi:10.1016/j.carbpol.2006.07.025

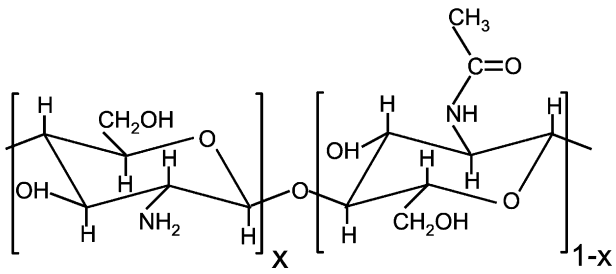

Scheme 1. Simplified chemical structure model for chitosan (with a deacetylation degree of X = DAD = 0.89) structural unit studied in this work and employed to calculate the molar composition of chitosan/glycerol blends.

chitosan as well as the source of the starting material, i.e. chitin. Really, commercial chitosan is a partially *N*-acetylated chitosan, i.e. a copolymer of glucosamine (GlcN) and *N*-acetylglucosamine (GlcNAc), whose structure is shown in Scheme 1. It is an amphiphilic macromolecule in which the ratio between acetylated and non-acetylated residues is responsible for the balance between hydrophilic and hydrophobic interactions. It has become of great interest not only as an underutilized resource, but also as a new functional material of high potential in various fields. Recent progress in chitin chemistry is quite noteworthy (Ravi Kumar, 2000).

Due to the presence of protonated amino groups chitosan exhibits polyelectrolyte character in dilute acid aqueous solution at low pH (below pH 6.5) and its hydrodynamic behaviour in solution is intricate (Wu, Zhou, & Wang, 1995). It is very well known, that the intrinsic viscosity $[\eta]$ of a polymer fraction in dilute solution is related to their average molecular weights through the Mark–Houwink–Sakurada–Staudinger equation: $[\eta] = K_n M_n^a = K_v M_v^a = K_w M_w^a$, the value of the exponent a may be also indicative of the stiffness of the macromolecule in solution. Thus, for very stiff macromolecules (rigid rods) the value of a approximates to 0.8–1.2 (Bohdanecký & Kovár, 1982; Moore, 1967). A very exhaustive compilation of a values has been done by Knaul, Kasaai, Bui, and Creber (1998) (Knaul et al., 1998) and the experimental results of some other authors (Berth, Dautzenberg, & Peter, 1998; Ravi Kumar, 1999; Ravi Kumar, 2000) have confirmed also this assumption for chitosan. The stiffness of macromolecules must yield to a high value of their glass transition temperature T_g.

Although some studies have indicated that chitosan has a low content of crystalline regions in its structure, some other authors prefer to call it fairly amorphous (Genta, Pavanetto, Conti, Giunchedi, & Conte, 1995; Portero, Remunan-López, & Vila-Jato, 1998; Struszczyk, 1987). In fact, WAXD patterns recorded by a high number of authors (Guan, Liu, Zhang, & Yao, 1998; Ikejima & Inoue, 2000; Ratto, Chen, & Blumstein, 1996; Singh & Ray, 1998) have shown the common fact of two amorphous halo rings centered at around ~10 and ~20 2θ degrees which are characteristics of short-range order structures.

Exploring the literature, it can be concluded that there exists a great debate about the glass transition temperature of chitosan. Glass transition temperature for chitosan have been reported previously by several authors, thus for instance among many of them, Sakurai, Maegawa, and Takahashi (2000) who reported a value of 203 °C as determined by DSC and dynamical mechanical thermal analysis (DMTA). Shantha and Harding (2002) reported a value of 195 °C while Dong, Ruan, Wang, Zhao, and Bi (2004) give a lower value of 140–150 °C by using four different techniques, namely, DSC, DMTA, thermally stimulated current spectroscopy (TSC) and dilatometry (DL). Most recent studies carried out by Cervera et al. (2004) found the T_g of chitosan by DSC measurement as 130–139 °C. Suyatma, Tighzert, and Copinet (2005) have observed, using different techniques, values for the T_g at around 194 and 196 °C. Other works (Pizzoli, Ceccorulli, & Scandola, 1991) situated the T_g above the degradation temperature. Whereas the investigations of other authors lead to lower values, thus for instance: Cheung, Wan, and Yu (2002) found it to be at around 103 °C; Toffey and Glasser (2001) which attributed the T_g of chitosan to the α-relaxation obtained by DMTA varying between 60 and 90 °C, in agreement with Lazaridou and Biliaderis (2002).

When the T_g of a polymer cannot be directly estimated, its blending with a low molecular weight substance, which depresses the T_g by a plasticizing effect, has been successfully employed. For this aim, we have blended chitosan with glycerol (1,2,3-propantriol) which is a model low molecular weight glass-forming liquid. We have chosen this molecule for several reasons. One of them is that the transitional behaviour of glycerol is well known (Arndt, Stannarius, Gorbatschow, & Kremer, 1996; Böhmer & Hinze, 1998; Korus, Hempel, Beiner, Kahle, & Donth, 1997; Reinsberg, Qiu, Wilhelm, Spiess, & Ediger, 2001; Schiener, Chamberlin, Diezemann, & Böhmer, 1997). And another reason to used glycerol as a plasticizer for chitosan is that its high boiling point and hydrogen bond ability causes a high retention in the polymer. Glycerol has been used to modify other natural macromolecules, for instance to increase the mobility of proteins (Zhang, Burgar, Do, & Lourbakos, 2005) to form gelatin films (Thomazine, Carvalho, & Sobral, 2005) maize starch (Mathew & Dufresne, 2002) or in cellulose films (Xiao, Zhang, Zhang, Lu, & Zhang, 2003). Glycerol may improve the processability of chitosan, and the mechanical properties of chitosan film (Suyatma et al., 2005). Thus, glycerol has been employed to increase the flexibility of keratin–chitosan composite films (Tanabe, Okitsu, Tachibana, & Yamauchi, 2002), and chitosan/glycerol films has been employed in controlled release devices (Brown et al., 2001). Other interesting questions to be explored in the present system chitosan/glycerol are the study of local motions and above all their sensitivity to small molecules such as glycerol. There are several works previously published on the matter such as for example on starch (Lourdin, Coignard, Bizot, & Colonna, 1997; Lourdin, Bizot, &

Collonna, 1997; Lourdin, Ring, & Colonna, 1998; Lourdin, Colonnna, & Ring, 2003; Partanen, Marie, MacNaughtan, Forssell, & Farhat, 2004).

In this paper, dynamic mechanical thermal analysis (DMTA) was employed to provide information about mechanical and relaxational behaviour of chitosan and its blends with glycerol, thus information may be compared with the thermal transitions observed by differential scanning calorimetry (DSC). Solid-state NMR spectroscopy is a powerful technique which provides information about the molecular dynamics of different components in a blend. Thus, it has been employed in the case of mixtures of a polysaccharide and a polyol (Cheung et al., 2002; Kruiskamp, Smits, Van Soest, & Vliegenthart, 2001; Smits, Hulleman, Van Soest, Feil, & Vliegenthart, 1999; Smits, Kruiskamp, VanSoest, & Vliegenthart, 2003; Zhang et al., 2005). Therefore, we have also used it. The information extracted from these three techniques will allow an understanding of the relationship of chitosan with this small molecule glass-forming liquid and an extrapolation of the molecular relaxations occurring in pure chitosan.

2. Experimental

2.1. Materials

The chitosan used in the present paper was a commercial sample obtained from Aziende Chimica e Farmaceutica (A.C.E.F.) S.p.a. Fiorenzuola D'Arda (Piacenza), Italy. This chitosan was obtained by deacetylation of chitin from fish shells. It had a degree of deacetylation of minimum 90.0% (manufacturer's specification). Glycerol, (Fluka Chemie, Buchs, Switzerland) was used as received as a solvent or plasticizer. Glacial acetic acid from Aldrich Chemicals. Purified deionized water from a Millipore Milli-U10 water purification facility was used where appropriate.

2.2. Average degree of deacetylation (DAD)

DAD can be estimated by ^{1}H NMR according Lavertu et al. (2003). Spectra were acquired on a Varian Mercury Unity 500 MHz spectrometer equipped with a 16 bits digitizer using a Varian 5 mm Indirect Detection probe in a 50% CF_3COOD/D_2O mixture (v/v) at 25 °C. The results indicate a DAD of the 89%.

In addition to the ^{1}H NMR experiments carried out, we have also carried out ^{13}C CP-MAS NMR solid-state experiments. The ^{13}C CP-MAS spectrum (does not shown here) corresponding to the films of chitosan shows two peaks at 24.2 and 180.1 ppm which following Toffey, Samaranayake, Frazier, and Glasser (1996) may be interpreted as due to methyl ($–CH_3$) and ionic *N*-acetate carbonyl groups ($–OOC–CH_3$), respectively. When chitosan is dissolved in acetic acid aqueous solution it gives the water-soluble ionic complex of chitosan and acetic acid, namely chitosoniun acetate, which can be handed like any other soluble linear polymer. However, on heating, let say 80–100 °C, it converts into chitin thus changing the composition of the respective structural unit ($NH^{+}_{3}{}^{-}OOC–CH_3 \overset{80–100\ °C}{\rightarrow} –NH–OC–CH_3 + H_2O$) (Toffey et al., 1996). It must keep in mind the changes of chemical structure on increasing the temperature above 100 °C. It may change the thermal and mechanical properties.

2.3. Pure chitosan and blended films preparation

Glycerol is a good glass former. Thus, for instance, there was no loss by evaporation of glycerol/chitosan films (GLY, bp = 290 °C) stored in a dry atmosphere at room temperature, which is in agreement with loss by evaporation tests of this plasticizer from chitosan/glycerol films carried out by Suyatma et al. (2005).

Films for DMTA and DSC measurements were prepared by the dissolve–drying method. Known amounts of chitosan were first dispersed in 1,2,3-propantriol (glycerol) at room temperature. Then an acetic acid aqueous solution containing 5% (wt/wt) acetic acid was added dropwise to the chitosan suspension. The suspension was stirred, usually after 12 h, until a clear viscous solution was obtained. The polymer in glycerol solution was poured into a six cavities poly(tetrafluoroethylene) (Teflon®) mould, and the films were first air dried for 48 h at room temperature and then in a high vacuum hot plate at 60 °C for 24 h at 10^{-3} mmHg to constant steady-state weight. The resulting films were collected and stored at room temperature and kept dry in a glass vacuum desiccator containing dry silica gel prior to use in each experiment. Strips for DMTA and DSC were punched off the films. All the films obtained by this procedure are in the non-neutralized form with the amino side groups protonated, i.e. as $–NH^{+}_{3}{}^{-}OOC–CH_3$ (quitosonium acetate) (Viciosa, Dionisio, Silva, Reis, & Mano, 2004).

2.4. Thermogravimetric effluent analysis by mass spectrometry (TGVA-MS)

TGA-MS thermograms of chitosan slabs were measured using a high resolution thermogravimetric analyzer TGA 2950 of TA Instruments (New Castle, DE, USA) used for qualitative analysis for unknown gas mixtures. It is hyphenated to a mass spectrometer VG Gaslab 300 of Gas Analysis-Fisons (Cheshire, UK) in order to distinguish between the different gas species. TGA was performed in the temperature range from 310 to 1000 K at a heating rate of 10 K min^{-1} in a purified dynamic nitrogen gas atmosphere (60 mL min^{-1}). The MS has a range of 300 amu (atomic mass units, m/z). A nitrogen purge of 50 mL min^{-1} was used in the furnace. The sample size of 11 mg was accurately weighed into an aluminium pan. Derivatograms of the TGA curves (DTG) were also recorded. In addition to the thermal stability provided by the thermogravimetric analysis, information about the decomposition products of chitosan may be obtained if the effluent gases are analyzed by means of a supplementary technique such as mass spectrometry (MS).

2.5. Differential scanning calorimetry (DSC)

DSC thermograms of chitosan small slabs were measured using a DSC from Perkin-Elmer, model DSC7, connected to a temperature controller and interfaced to a thermal analysis data station (TADS). Temperature and enthalpy calibration were checked with Indium ($T_m = 156.6$ °C, $\Delta H_m = 28.55$ J g^{-1}) and Gallium ($T_m = 29.9$ °C, $\Delta H_m = 80.14$ J g^{-1}). Well dried and free of water films were sealed in aluminum pans and heated at a rate of 10.0 K min^{-1}. All experiments were done under a purge of dry nitrogen at a rate of 50 mL min^{-1} during data collection.

2.6. Dynamic mechanical thermal analysis (DMTA)

Dynamic mechanical relaxations were evaluated with a Polymer Laboratories MK II Dynamic Mechanical Thermal Analyzer, working in the tensile mode. This means a sinusoidal force of known magnitude which is applied and the resultant displacement in the sample is measured. Typically a force of 0.05 N was applied. The storage modulus E', the loss modulus E'', and the loss tangent, $\tan\delta$, of each sample were obtained as a function of temperature over the range from 140 to 400 K at fixed frequencies of 1, 3, 10 and 30 Hz and at a $R_H = 1.5$ K min^{-1}. The specimens used were rectangular strips 3 mm wide, around 0.3 mm thick, and over 10 mm in length. Some other details have been given elsewhere (Quijada-Garrido, Barrales-Rienda, Pereña, & Frutos, 1997).

2.7. Solid-state NMR measurements

^{1}H magic angle spinning (MAS), ^{13}C cross-polarization (CP) and high power decoupling (HPDEC) MAS NMR spectra were recorded on a Bruker Avance™ 400 spectrometer/imager (Bruker Analytik GmbH, Karlsruhe, Germany) equipped with a Bruker UltraShield™ 9.4-T (^{1}H resonance frequency of 400.14 MHz). The 90° pulse lengths were 5.3 and 3.3 μs for ^{13}C and ^{1}H, respectively. ^{13}C CP-MAS spectra were measured with 1 ms contact time, 30 kHz spectral width and up to 8000 scans. During the detection period of the ^{13}C magnetization, dipolar decoupling was used to eliminate the large ^{13}C–^{1}H heteronuclear dipolar decoupling. The chemical shifts ^{13}C spectra are referenced to TMS by using the methine carbon of solid adamantine (29.5 ppm) as an external reference standard. Proton spectra were measured with 100 kHz spectral width, 8 k data points and 64 accumulations. Selective $T^H_{1\rho}$ measurements were performed using a spin-lock pulse sequence with a delayed contact time. Variable ^{1}H spin-lock delays from 0.01 to 4 ms were used prior CP. $T^H_{1\rho}$ were calculated from: $M_t = M_0 e^{-1/T^H_{1\rho}}$ where t is the spin-lock time used in the experiment, and M_0 and M_t are the peak intensities at zero and t times, respectively.

3. Experimental results

3.1. Thermal stability of chitosan

A TGA loss weight curve of chitosan and its derivative curve are shown in Fig. 1a. TGVA-MS data are given in Fig. 1b. Keeping in mind the mechanism of degradation of some other polysaccharides and some other analogous substances (Baker, Coburn, Liu, & Tetteh, 2005; Cardenas & Miranda, 2004; Kerwin, Whitney, & Sheikh, 1999;

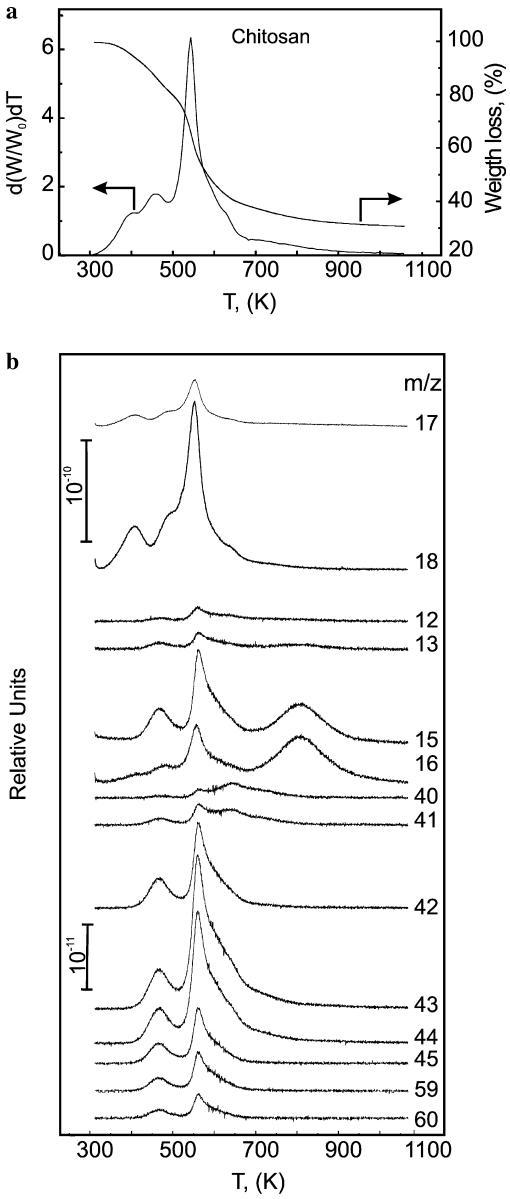

Fig. 1. (a) Thermal stability TGA curve of a purified chitosan sample (DAD = 89%) in a purified nitrogen atmosphere and at a rate of heating of $R_H = 10.0$ K min^{-1}. (b) Composition curves (TGVA) from mass spectrometry of effluents from TGA curve of the same purified chitosan. Only the most relevant peaks for simplicity are shown. Figures given on the right hand side represent m/z of a series of fragments produced during the thermal degradation of chitosan. For mass spectra interpretation see the text.

Murphy, 1962; Pappa, Mikedi, Tzamtzis, & Statheropoulos, 2003; Wanjun, Cunxin, & Donghua, 2005) and the mass spectrometric profiles of glucosamine, glucosamine trimer and glucosamine polymers (chitosan) it is very plausible to establish that chitosan sample degrades in a four or five stages process as can be seen from its DTGA curve. Cardenas and Miranda (2004) have found a similar DTGA pattern but with three or four stages process of degradation.

The first step probably is controlled by cross-linking reactions which occur by the elimination of small molecules from the functional groups in the glucopyranose ring. Therefore, the first stage has a maximum at $\sim$ 400 K with a weight loss of 11–14% which the TGA-MS data given in Fig. 1b, represents a weight loss of water. It may have two different origins, on the one hand, chemisorbed water through hydrogen bonds, and the other hand, water resulting from an elimination reaction or from $NH^+{}_3{}^-OOC{-}CH_3 \overset{80\text{–}100\ ^\circ C}{\rightarrow} {-}NH{-}OC{-}CH_3 + H_2O$. The mass spectrum of water show peaks that can be assigned to masses (m/z) of 18 ($[H_2O]^+$) and 17 ($[OH]^+$). Under nitrogen atmosphere, the thermal degradation of chitosan follows a random scission pathway initiated at the weak links (Zohuriaan & Shokrolahi, 2004). The second stage has a maximum at $\sim$460 K with a weight loss of 20–24% which from the TGA-MS data also given in Fig. 1b, represents a weight loss of methane 16 ($[CH_4]^+$), 15 ($[CH_3]^+$) and 13 ($[CH]^+$) and a weight loss of ammonia NH_3 from an elimination reaction between $-NH_2$ and $-H$ groups giving place to masses of 17 ($[NH_3]^+$), 16 ($[NH_2]^+$), 15 ($[NH]^+$) and 14 ($[N]^+$). Acetamide, probably from the chitosonium acetate $NH^+{}_3{}^-OOC{-}CH_3$ by an elimination reaction simultaneously with ammonia giving place to masses of 59 ($M^+ = [CH_3CONH_2]^+$), 44 ($M^+ - [CH_3]^+$), 43 ($M^+ - [NH_2]^+$), 42 ($M^+ - [NH_3]^+$), 41($M^+ - [NH_4]^+$or /and $[H_2O]^+$), 18 ($[H_2O]^+$ or/and $[NH_4]^+$), 15 ($[CH_3]^+$). And acetic acid giving place to masses of 60 ($M^+ = [CH_3COOH]^+$), 45 ($M^+ - [CH_3]^+$), 43 ($M^+ - [OH]^+$), 42 ($M^+ - [H_2O]^+$) and 15 ($[CH_3]^+$).

Latter on, generally in polysaccharides, dehydration, depolymerization and pyrolytic decomposition of the backbone are involved at these high temperature stages resulting in the formation of H_2O, CO and CH_4, and in the case of chitosan, NH_3 (Zong, Kimura, Takahashi, & Yamane, 2000). In fact, the third stage has a maximum at 533 K with weight loss of 35–40% which represents the decomposition of the main chain with the production of H_2O, CO and CO_2 and some others fragment from the glucosaminic ring, namely, 12 ($[C]^+$), 16 ($[O]^+$), 17 ($[OH]^+$), 18 ($[H_2O]^+$) and 44 ($[CO_2]^+$). And a fourth one probably originated by the formation of a carbonaceous residue from the remaining degraded structures, with a maximum around 630 K, and the formation of hydrogen cyanide with a m/z of 27 ($[HCN]^+$), which can also come from purge nitrogen, i.e. 27 ($[N_2]^+$) and acetonitrile with a m/z of 41 ($[CH_3CN]^+$), 40 ($[CH_2CN]^+$) and 39 ($[CHCN]^+$). And the fifth one with a maximum around 800 K, with the formation of methane with a m/z of 16 ($[CH_4]^+$), 15 ($[CH_3]^+$) and 13 ($[CH]^+$). This TGA-MS analysis confirms again the special care which must be taken on heating chitosan specimens obtained by evaporation from acetic acid aqueous solutions.

3.2. Differential scanning calorimetry of chitosan/glycerol blends

DSC thermograms of chitosan and their mixtures with glycerol are shown in Fig. 2. The DSC trace corresponding to pure chitosan does not show any transition which could be attributed to the glass transition. We can observe during the heating of the sample a change in the trend of the baseline which may be due to an elimination of water strongly adsorbed (chemisorbed water through hydrogen bonds). For this reason some authors have located in this region the glass transition temperature T_g of chitosan by DSC. Above this temperature, degradation processes start as it was shown in the last section. For pure glycerol, a second order transition at 192 K appears, which agrees quite well with the glass transition temperature T_g of glycerol reported by different authors (Angell, 1984; Götze & Sjögren, 1992; Hansen & Richert, 1997; Masciovecchio et al., 1998; Reinsberg et al., 2001; Ryabov, Hayashi, Gutina, & Feldman, 2003; Sokolov, Kisliuk, Quitmann, Kudlik, & Rössler, 1994; Sokolov, Steffen, & Rössler, 1995). In DSC thermograms corresponding to chitosan/glycerol mixtures shown in Fig. 2, a transition at low temperature appears at the T_g region of glycerol, this transition moves to higher temperature as the chitosan in the mixtures increases, at the same time the transition smoothes, so that, it is hardly noticed for the enriched chitosan blends. The influence of the composition on this transition is shown

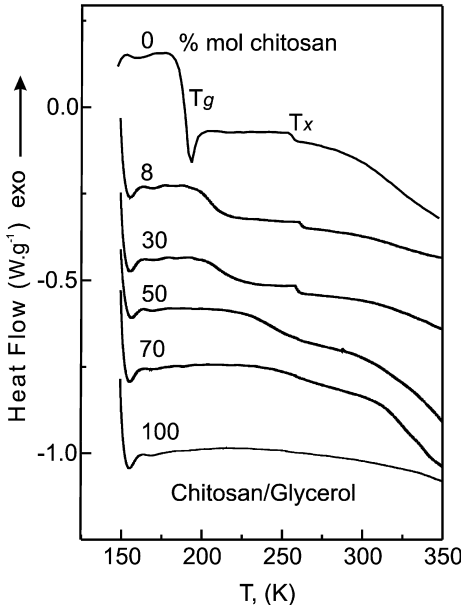

Fig. 2. Differential scanning calorimetry (DSC) curves for chitosan/glycerol blends at different concentrations in a purified nitrogen atmosphere and at a rate of heating of $R_H = 10.0$ K min^{-1}.

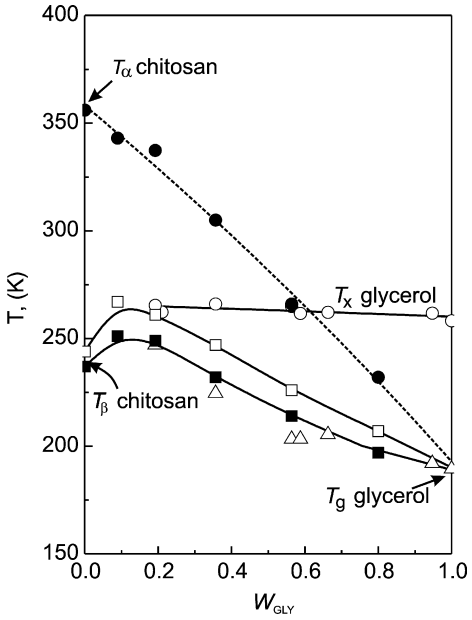

Fig. 3. Plots of the thermal transitions and relaxations of chitosan, 1,2,3-propantriol and their blends against composition (W_{GLY}). Differential scanning calorimetry data (DSC): (○) second scaling temperature T_x in the MCT model; (Δ) glass transtion temperature T_{gGLY} in the chitosan/glycerol blends. Dynamic mechanical thermal analysis data (DMTA): (●) $T_{(\alpha)}$ relaxation temperature from tan δ of chitosan, glycerol and their blends. (■) β-Relaxation temperature from E″ in the chitosan/glycerol blends and (□) β-relaxation temperature from tan δ in the chitosan/glycerol blends. Dashed line (----) represents the fitted line to the experimental data by means of the Gordon–Taylor–Wood's equation. Each data point represents at least the means of three replicate determinations under identical experimental conditions.

in Fig. 3. The data of heat flow (W g^{-1}) against temperature (T), shown in Fig. 2 for glycerol and chitosan/glycerol blends reveal a well common developed onset at ~258–266 K. This transition is a subject of special interest. When these values are plotted against % wt glycerol content (Fig. 3), we can see that it does not show any appreciable dependence on composition. Therefore it may be considered as a transition due to the glycerol molecule alone. Ryabov et al. (2003) have performed DSC measurements of anhydrous glycerol for the temperature interval from 133 up to 303 K (Ryabov et al., 2003). They found the T_g at 190 K and a quite distinguishable change in the sample heat capacity at 263 K. Ryabov et al. (2003) have explained it according the mode-coupling theory (MCT), which predicts a dynamic phase-transition temperature from solid-like to liquid-like (amorphous) behaviour at some critical temperature T_c, which is located well above T_g.

This transition above T_g has been also found in the case of polymer additives of high molecular weight (Wu et al., 2000; Wu, 2001) and it has also considered as a phase transformation from a true liquid state to a liquid, which is fixed by hydrogen bonds between hydroxyl groups within the additive. It constitutes a highly ordered phase. When the additive was blended with chlorinated polyethylene (XCPE), Wu et al. (2000) reported a novel transition which appeared above the glass transition temperature of the additive. In this case it has been assigned to the dissociation of strong intermolecular hydrogen bonds between the polymer and additive within the additive rich phase (Wu, 2001).

3.3. Relaxation processes of chitosan/glycerol blends

Fig. 4 shows the plots of the storage (E') and loss moduli (E'') and the loss tangent, tan δ as a function of temperature for our chitosan sample at 1, 3, 10 and 30 Hz. Clearly three relaxation processes appear namely at low temperature, the β-relaxation, with activation energies of 98 kJ mol^{-1}, and at higher temperature two overlapped processes, the α- and α′-relaxation with activation energies of 262 and >400 kJ mol^{-1}, respectively. It is noteworthy that activation energies determined from peak maxima in temperature domain measurements may differ from those determined in frequency domain due to shape of $E''(\omega, T)$ surface. For sharp relaxation peaks this effect is small but for broad β-relaxations the differences can be large.

Fig. 5 displays one of the series experimental DMTA data of tan δ, against temperature T at 1 Hz for the chitosan/glycerol blends. In theses samples at least two relaxations could be distinguished. The position of their maxima is clearly depending on composition. Looking at the tan δ spectrum corresponding to the highest glycerol content blend (8% mol chitosan), a sharp relaxation about

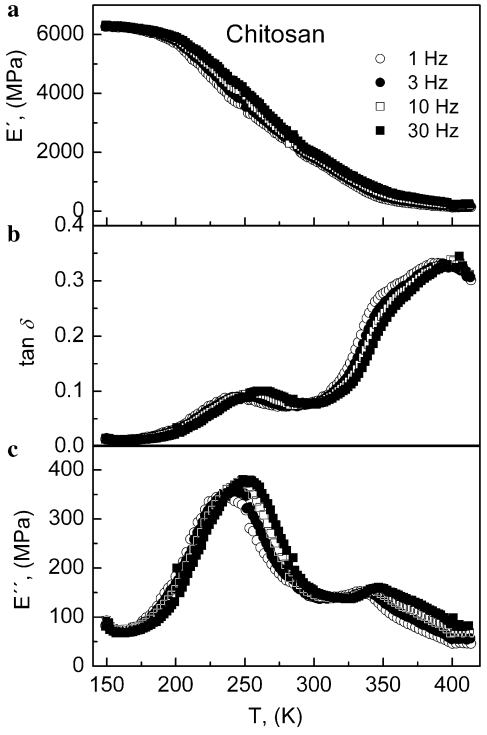

Fig. 4. Dynamic mechanical thermal analysis data (DMTA) for chitosan. Temperature dependence of: (a) storage modulus E'; (b) loss tangent, tan δ; and (c) loss modulus E'', at fixed frequencies of 1, 3, 10 and 30 Hz and at a $R_H = 1.5$ K min^{-1}.

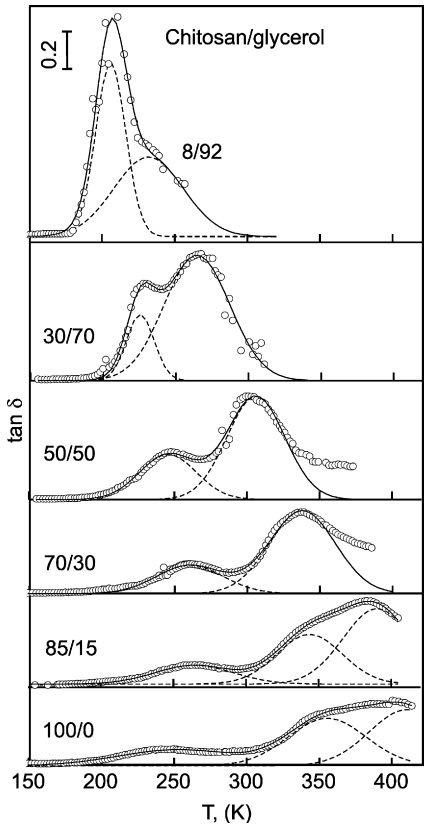

Fig. 5. Dynamic mechanical thermal analysis data (DMTA) for chitosan/glycerol blends. Temperature dependence of the loss tangent, tan δ at a frequency of 1 Hz and a rate of heating $R_H = 1.5$ K min^{-1}.

206 K at 1 Hz occurs. This transition agrees quite well with the calorimetric T_g (189.4 K) of pure glycerol shown in Fig. 2. The temperature of the maximum of the α-relaxation of chitosan, which we have attributed to the glass transition, decreases with increasing glycerol content, suggesting a plasticizing effect on the chitosan. At the same time, the low temperature relaxation attributed to glycerol moves to higher temperature when the polymer content increases, being it indicative of a decrease of the glycerol mobility. Both relaxations have been separated by deconvolution. There is not a theoretical basis that can satisfactorily explain the shape of the dependence of tan δ on temperatures although some factors that can influence it are known. Rotter and Ishida (1992) have applied a method of curve deconvolution to analyse the dynamic mechanical loss tangent in the region of the glass transition of several polymers, confirming the validity of this empirical approximation, besides to check that the Gaussian function furnished the best fitting. There are described in the literature other series of cases in which the Gaussian function had also provided the best fitting using experimental data from several techniques of analysis, as can be the torsional braid analysis (Gillham, Benci, & Boyer, 1976), torsion pendulum (Jacoby, Bersted, Kissel, & Smith, 1986), DMTA (Quijada-Garrido et al., 1997), dielectric measurements (Fuoss, 1941; Quijada-Garrido et al., 1997), and dilatometry (Enns & Simha, 1977). This may be suggesting that this type of curve is inherent to the relaxation process and not the measurement method. As illustrated in Fig. 5, the Gaussian function employed with the aid of a computer program (Origin® 7.0, SRO OriginLab Corporation, One Roundhouse Olaza, Northampton, MA, USA) provides a very good overall fitting to the whole range of tan δ versus T data. The maxima of the loss tangent tan δ at 1 Hz are plotted in Fig. 3 and their values given in Table 1, as well as the activation energies of the processes. The apparent activation energy values were calculated from the frequency shift of the temperature according to the Arrhenius-type equation. In Fig. 3 calorimetric and DMTA results are compiled. It is observed that the calorimetric glass transition temperature attributed to glycerol in the mixtures (Δ) agrees quite well with the β-relaxation temperature in the chitosan/glycerol blends obtained from E″ (■), whereas β-relaxation temperature in the chitosan/glycerol blends from tan δ leads to higher temperatures (□).

The glass transition depression for the chitosan (α-relaxation), illustrated in Fig. 3 as full circles, can be modelled by using the empirical Gordon–Taylor–Wood (GTW) (Gordon & Taylor, 1952; Wood, 1958) equation which has proved to describe many other plasticized systems. The equation of GTW (Gordon & Taylor, 1952; Wood, 1958) may be written as follows:

$$T_g = \frac{(W_{GLY} T_{gGLY} + k \cdot W_{CHI} T_{gCHI})}{W_{GLY} + k \cdot W_{CHI}} \quad (1)$$

Table 1
Dynamic mechanical relaxations of chitosan and some of their chitosan/glycerol blends at a series of frequencies, values obtained from tan δ

Composition (% mol chitosan)	T_{max} (K)									
	T_α				E_a (kJ mol^{-1})	T_β				E_a (kJ mol^{-1})
	1 Hz	3 Hz	10 Hz	30 Hz		1 Hz	3 Hz	10 Hz	30 Hz	
100	358	362	367	372	262	243	250	257	261	98
85	336	341	347	353	192	266	269	272	276	211
70	337	339	341	346	374	260	264	268	272	176
50	305	312	318	323	156	247	250	252	255	222
30	265	270	276	279	151	225	227	230	234	166
8	231	235	238	244	130	206	208	211	214	171

where $k = (\alpha^{l}_{CHI} - \alpha^{g}_{CHI})/(\alpha^{l}_{GLY} - \alpha^{g}_{GLY}) = \Delta\alpha_{CHI}/\Delta\alpha_{GLY}$, and W_{GLY} and W_{CHI} are weight fractions of glycerol and chitosan, respectively and T_{gGLY}, T_{gCHI} and T_g are the glass transition temperatures of glycerol, chitosan and of their mixtures or blends, respectively. And $\Delta\alpha_{CHI}$ and $\Delta\alpha_{GLY}$ are the differences for the thermal expansion coefficients in the liquid and in the glassy state of chitosan and glycerol, respectively. Since the thermal expansion coefficients are unknown to us, k must be considered as a whole and for this reason as an adjustable empirical parameter. Therefore, if T_gs for a series of mixtures and their respective mixture composition are known, T_{gGLY}, T_{gCHI} and k may be obtained as adjustable parameters. In fact, from T_g (T_α at 1 Hz) values as a function of composition given in the Table 1 for chitosan/glycerol blends the fitting to Eq. 3 yields to the following values for the adjustable parameters: $T_{gGLY} = 192.9$ K, $T_{gCHI} = 358.2$ K and $k = 1.16$. The dashed line curve given in Fig. 3 has been calculated with these parameters. A determination coefficient $R^2 = 0.9923$ indicates the goodness of the fitting.

3.4. Solid-state NMR

The broadening of proton lines in rigid solids is caused by homonuclear dipolar coupling. This phenomenon has long been used to obtain information on molecular dynamics in polymer and other organic materials. Molecular mobility averages these couplings and thus reduces the line width. Motions with rates exceeding the dipolar coupling of protons (typically 50 kHz) are detected through the reduction of the static dipolar line broadening. This has been exploited in ^{1}H wide line spectroscopy to reveal information about the molecular dynamics of different components in a blend (Quijada-Garrido, Wilhelm, Spiess, & Barrales-Rienda, 1998; Radloff, Boeffel, & Spiess, 1996). Fig. 6 shows ^{1}H MAS NMR spectra at 5 kHz corresponding to pure chitosan and some of its blends with glycerol. As it is easily seen there are differences in the mobility of these samples, which is related to the differences in their glass transition temperatures. For 8 and 30% mol chitosan very narrow signals are observed, a decrease in mobility is appreciated for 50% mol chitosan and for 70, 85 and 100% mol chitosan very broad signals are recorded indicating a strong decrease in the mobility.

In Fig. 7 ^{13}C CP-MAS NMR spectra corresponding to chitosan and several of chitosan/glycerol blends are shown. ^{13}C CP-MAS NMR spectra give information about the structure and composition. Cross polarization enhances the signal from the most rigid region of the sample. In Table 2, chemical shifts corresponding to the samples plotted in Fig. 7 are collected; it can be observed that there are not changes on chemical shift for the series of samples. The two signals corresponding to glycerol at 63.9 and 73.3 ppm are well resolved for 30 and 50% mol chitosan samples, suggesting that strong intermolecular interactions between chitosan and glycerol may occur, fact that would lead to a decrease in the mobility of glycerol and would cause an

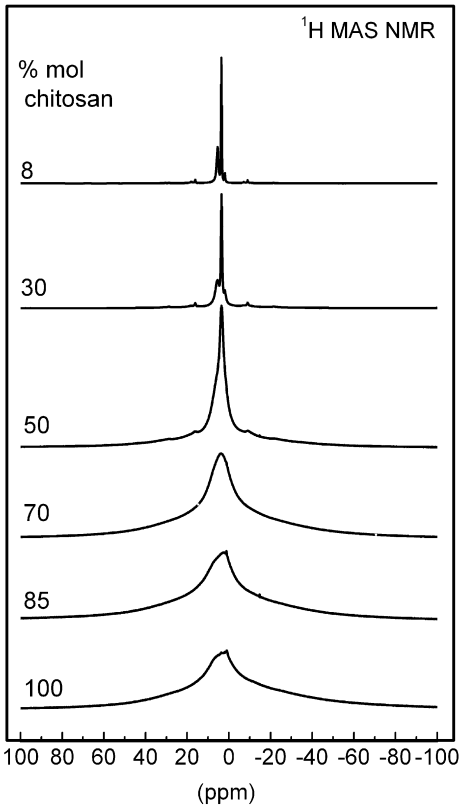

Fig. 6. ^{1}H MAS NMR spectra at 298 K of pure chitosan and 8, 30, 50, 70 and 85% mol chitosan in chitosan/glycerol blends.

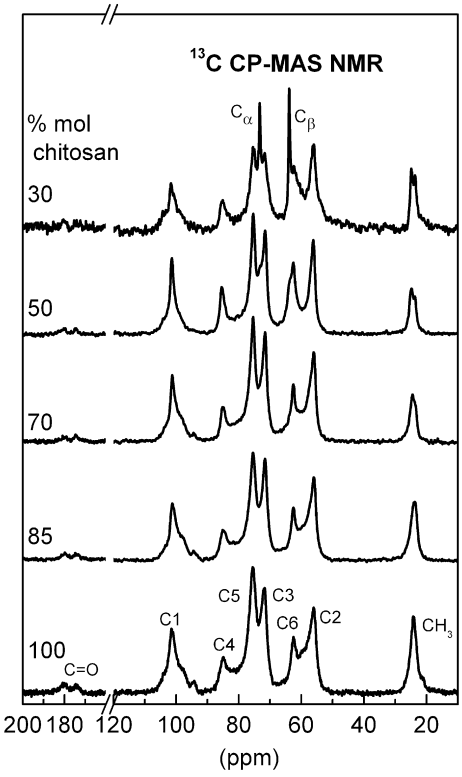

Fig. 7. ^{13}C CP-MAS NMR spectra at 298 K of pure chitosan and 30, 50, 70 and 85% mol chitosan in chitosan/glycerol blends.

Table 2
Chemical shifts of chitosan/glycerol blends obtained by ^{13}C CP-MAS NMR

	Composition (% mol chitosan)				
	100	85	70	50	30
C_1	101.4	101.0	101.2	101.4	101.6
C_2	56.1	56.0	56.2	56.4	56.2
C_3	71.9	71.6	71.7	71.6	71.7
C_4	85.0	84.9	84.9	85.3	85.0
C_5	75.5	75.5	75.5	75.4	75.3
C_6	62.5	62.6	62.5	62.5	62.5
CH_3	24.2	24.0	23.5/24.5	23.7/24.9	23.7/24.9
CO	180.1/174.5	179.6/173.9	174.5/179.7	174.4/179.9	174.5/180.1
C_α	–	–	–	72.9	73.3
C_β	–	–	–	63.8	63.9

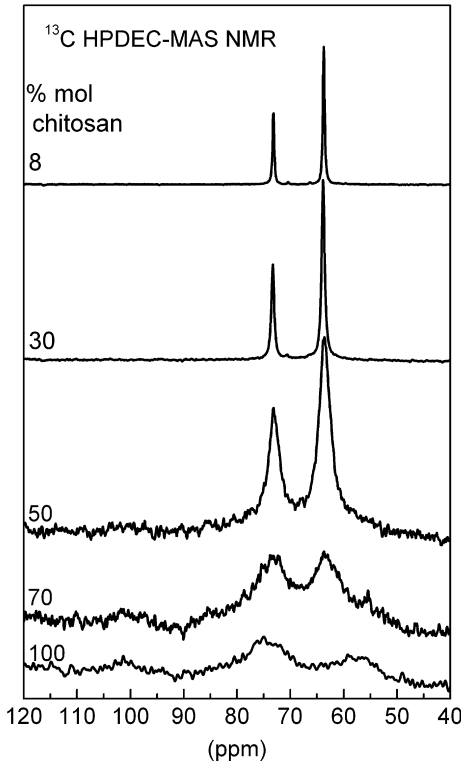

Fig. 8. ^{13}C HPDEC-MAS NMR spectra at 298 K of pure chitosan and 8, 30, 50 and 70% mol chitosan in chitosan/glycerol blends.

effective cross-polarization between ^1H and ^{13}C within glycerol molecules, or between ^1H in chitosan to glycerol ^{13}C. ^{13}C CP-MAS spectrum corresponding to the blend with 8% mol chitosan had not been shown because the signal was too low, indicating the strong increase of the mobility in the sample.

In Fig. 8 direct polarization ^{13}C HPDEC-MAS spectra corresponding to chitosan/glycerol blends are presented. With this technique only mobile parts of the sample are detected. It can be seen that the main signals in the spectra correspond to glycerol, lines become narrower with increasing glycerol content in the sample. The broadening of the lines for high chitosan content may indicate the interactions between glycerol and chitosan.

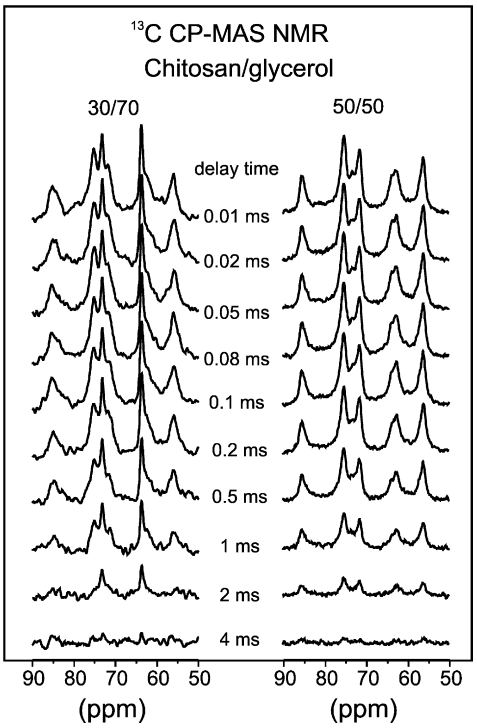

Fig. 9. ^{13}C CP-MAS NMR spectra corresponding to the proton spin-lattice relaxation time in the rotating frame $T_{1\rho}^{H}$ measurements, as a function of the delay time at 298 K of 30, and 50% mol chitosan in chitosan/glycerol blends.

To get a deep insight into the interaction between chitosan and glycerol, measurements for the two samples with 50 and 30% mol chitosan have been carried out. Fig. 9 shows ^{13}C CP-MAS NMR spectra corresponding to the proton spin-lattice relaxation time in the rotating frame $T_{1\rho}^{H}$ measurements, as a function of the delay time at 298 K of 30, and 50% mol chitosan in chitosan/glycerol blends. As it can be observed, for the 50% mol blend, the intensity decreases at the same time for all the signals with an increasing delay time, which indicates that the blend is homogeneous at the scale of the spin diffusion path length within $T_{1\rho}^{H}$ time, namely a few nanometers. On the contrary for the 30% mol blend, the intensity of the two signals at 63 and 74 ppm corresponding to glycerol, shows slightly lower decrease than the signal intensity corresponding to chitosan. For 50% mol sample a $T_{1\rho}^{H}$ of 1.2 ms has been estimated, whereas for the 30% mol blend a $T_{1\rho}^{H}$ of 1.3 ms has been obtained for chitosan and a $T_{1\rho}^{H}$ of 1.9 for glycerol.

4. Discussion

It may assume that relaxation processes in chitosan would be comparable with those occurring in other polysaccharides (Biliaderis, Lazaridou, & Arvanitoyannis, 1999; Einfeldt, Meißner, & Kwasniewski, 2001, 2003, 2004; Kalichevsky, Jaroszkiewicz, Ablett, Blanshard, & Lillford, 1992; Kalichevsky, Jaroszkiewicz, & Blanshard, 1992; Kelley, Rials, & Glasser, 1987; LeMeste, Roudaut, & Davidou, 1996; MacInnes, 1993; Meißner, Einfeldt, &

Kwasniewski, 2000; Meißner, Einfeldt, & Einfeldt, 2001; Montès, Cavaillé, & Mazeau, 1994; Ratto et al., 1996; Simatos, Blond, & Perez, 1995; Sperling, 1986). Einfeldt and coworkers (Einfeldt et al., 2001, Einfeldt, Meißner, & Kwasniewski, 2003, 2004; Meißner et al., 2000; Meißner et al., 2001) have widely investigated the relaxation processes occurring in cellulose and other polysaccharidic materials by means of dielectric spectroscopy. The assignation of the different relaxation processes in these biopolymers seems intricate. Einfeldt and coworkers attributed the main dominant relaxation process at low temperature, the β-relaxation, to local chain (o segmental motion), contrary to Montès et al. (1994) who attributed this low temperature relaxation to lateral side-group motions. Two main arguments supported this hypothesis (Meißner et al., 2000; Meißner et al., 2004): on one hand they found that β-relaxation not only occurs in cellulose but also in dextran, which has no methylol side-groups, and on the other hand they did not found the β-relaxation in monomers as glucose and arabinose, because the glucosidic linkage is absent in the monomers. However, Chan, Pathmanathan, and Johari (1986) have found by dielectric spectroscopy that glucose have a well developed β-relaxation, therefore this fact invalidates one of these two last arguments.

In chitosan, the presence of a $-NH_2$ ionisable group has to be considered. Viciosa and coworkers (Viciosa et al., 2004; Viciosa, Dionisio, & Mano, 2006) have investigated the dielectric relaxation behaviour of neutralized and non-neutralized chitosan, three relaxation processes for chitosan were detected, a β-wet process, when the sample had a high water content, that vanishes after heating to 150 °C, a β-process located below 0 °C, that becomes better defined after annealing at 150 °C and a σ-process that deviates at higher temperature with drying. In dried neutralized chitosan a fourth process was observed in the low frequency side of the β-relaxation.

Toffey and Glasser (2001) have performed dynamical mechanical thermal analysis of ionic complexes of chitosan with some alkanoic acids and of the amidized homologous of chitosan. The β-relaxation observed at low temperature was enhanced for the ionic complexes and it was attributed to side group motions. This relaxation is enhanced in the ionic complexes compared to the amidized form, this fact was attributed to the presence of residual free acid acting as a plasticizer.

As we have seen the discrepancies occurring in the assignation of the low temperature relaxation in polysaccharides and in chitosan, the assignation of the T_g is also a matter of debate (Kaymin, Ozolinya, & Plisko, 1980; Ogura, Kanamoto, Itoh, Miyashiro, & Tanaka, 1980; Pizzoli et al., 1991; Toffey & Glasser, 2001). For instance, Pizzoli et al. (1991) have attributed the two relaxation processes found in mechanical measurements to local motions, the high temperature relaxation was not interpreted as the glass transition, due to the activation energy they found, about 100 kJ mol^{-1}, too low for a cooperative process, they located the T_g above the degradation temperature of chitosan. Guan et al. (1988) have found by DMTA two relaxations at 378 and 218 K, which they assigned to α- and β-relaxations, respectively, but they did not interpreted their molecular origin. Ratto et al. (1996) found three relaxations for chitosan samples annealed up to 180 °C, they found the relaxations were depending on the thermal treatment and were attributed to local motions. Toffey and Glasser (2001) also found two relaxation they called β- and α-relaxations. The α-relaxation appeared around 60–93 °C depending on the acid used to prepare the chitosan films, which they attributed to the T_g of chitosan.

All these discrepancies could be due to the different preparation of the chitosan films, the acid used for the film formation, the degree of neutralization, when it is neutralized, and the thermal treatment employed. In some instances high temperatures have been used to dry the sample, which may give place to an appreciable change of chemical structure and/or degradation within the material. Thus and coming back to the a'-relaxation, found in pure chitosan and in the blend with the highest chitosan content, we think that this relaxation can be attributed to the transformation of chitosonium acetate units, formed during the film preparation, into chitin. Toffey et al. (1996) observed that DMTA transitions occur at increasingly higher temperatures, and over progressively wider temperature ranges, as the transformation progresses in successively scans.

The presence of water and/or plasticizers modifies the relaxation spectrum of a polymer. In the present work, it has been observed that glycerol has a great influence on the relaxation appearing at high temperature, moving to lower temperature with increasing glycerol in the mixture, this dependence with composition has been modelled by the GTW equation (Gordon & Taylor, 1952; Wood, 1958). Due to the cooperativity of this process and the plasticization effect, we suggest that this relaxation correspond to the T_g of chitosan as Toffey and Glasser (2001) proposed. By means of ^1H MAS NMR the line narrowing of the blends with increasing glycerol content is also indicative of a decrease of the T_g. Due to the stiffness of the chitosan backbone and its own configuration, the glass transition must be interpreted as torsional oscillations between two glucosamine rings across glucosidic oxygens and a cooperative hydrogen bonds reordering. This effect will also explain the high values found for the activation energies for this transition as it is shown in Table 1. The relatively high activation energy values found are indicative of large degree changes in segmental mobility and a high degree of cooperativity enhanced by the participation of inter and intramolecular hydrogen bonds assemblies. There exists a class of polymers having unusual configurational characteristics (Barrales-Rienda & Pepper, 1966; Economy, Storm, Matkovich, Cottis, & Nowak, 1976; Romero Colomer, Meseguer Dueñas, Gomez Ribelles, Barrales-Rienda, & Bautista Ojeda, 1993) as well as torsional potentials (Erman, Flory, & Hummel, 1980; Hummel & Flory, 1980). In these polymers, the molecular mobility of a series

of rings with a single interconnecting functional group or atom is determined by the torsional oscillation motion.

Our results are in agreement with that found for others authors in blends of chitosan and other polysaccharides with low molecular weight substances (Kaymin et al., 1980; Lazaridou & Biliaderis, 2002). Lazaridou and Biliaderis (2002) (Lazaridou & Biliaderis, 2002) have found two relaxations in chitosan, the highest temperature relaxation, they called α- relaxation and assigned to the T_g, which decreases in temperature by incorporation of sorbitol and/or moisture. The relationship between the T_g and moisture was also modelled with the GTW equation, an activation energy between 225 and 544 kJ mol^{-1}, that is a cooperative process. They estimated the T_g of chitosan around 370 K, in agreement with the value reported in the present contribution.

For the low temperature relaxation, we found more plausible that it is due to local motions of the side chains in chitosan. In presence of glycerol, the β-relaxation has been attributed to glycerol interacting with chitosan through hydrogen bonding between alcoholic and amine lateral groups from chitosan and glycerol alcoholic groups. Zhang, Burgar, Lourbakos, and Beh (2004) have found a β-relaxation at −60 °C in wheat proteins and polyvinyl alcohol blends with glycerol, they attributed this relaxation to the glass transition of bound water and glycerol strongly associated with the polymer matrix through hydrogen bonding. These hydrogen bond assemblies between chitosan and glycerol affect the temperature and activation energy of this relaxation. As the glycerol concentration is increased the cooperativity increases and the relaxation moves towards the T_g of pure glycerol. The effective interaction between chitosan and glycerol have been revealed by the decreasing of glycerol mobility observed in the ^{13}C HPDEC-MAS experiment and the glycerol signals appearing in the ^{13}C CP-MAS experiment. In Fig. 3 a plot of the β-relaxation and the glass transition of chitosan and glycerol, respectively, and their blends have been plotted as a function of composition. As we can see it represents a strong dependence of the thermal transition temperatures against composition. From the qualitative point of view, having a look on this Fig. 3, the introduction of increasing amounts of the hydrogen bond (glycerol) component in the blend results, first, in a soft increase in the intermolecular hydrogen bond (chitosan/glycerol) and therefore in the thermal transition. Second, an accentuated diminution on the transition reflected in the shape of the β-relaxation versus composition because an increment of the glycerol–glycerol intermolecular hydrogen bonds. This suggests an overall inversion of the hydrogen bond interactions in the blends. In fact this effect must be due not only to a change of composition but to a change of the kind of the hydrogen bond interactions. It represents and can be described as a balance among intra and intermolecular hydrogen bonds in chitosan and glycerol. At the very beginning the hydrogen bonds balance is predominantly determined by intramolecular interactions in chitosan.

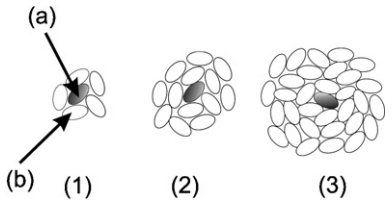

Fig. 10. Bidimensional model for the formation of "clusters" by hydrogen bonds between chitosan and glycerol molecules among them. (a) Glycerol molecules are directly bonded to chitosan through –NH_2 or –$NH^+{}_3{}^-$OOC–CH_3 (quitosonium acetate), –CH_2OH and in some extension –NH–CO–CH_3, functional groups forming a hydrogen bonded anchoring place to the glycerol "clusters". (b) Glycerol molecules hydrogen bonded to some other glycerol molecules through –CH_2OH alcoholic groups in glycerol forming a hydrogen bonded network ("cluster"). (1), (2) y (3) represents growing size of the clusters with glycerol concentration in the blend.

On the basis of a qualitative analysis of all effects described above, we will propose a consistent model of the clusters formed on a chitosan surface by a glass-forming liquid such as glycerol. It can be described qualitatively by means of the simple model depicted in Fig. 10. For samples with a high glycerol concentration, namely in the vicinities of pure glycerol, –NH_2 or as –$NH^+{}_3{}^-$OOC–CH_3 (quitosonium acetate), –CH_2OH and in some extension –NH–CO–CH_3, groups form intermolecular hydrogen bonds with –CH_2OH alcoholic groups from glycerol on one hand. This leads to strong interactions between matrix (chitosan) and glycerol molecules, restricting the motion of this glycerol molecule. But, on the other hand, these alcoholic groups in polyhydroxylated molecules such as glycerol can also form hydrogen bonds among them thus giving place to a clustering effect. The process resembles and likely resulting in plasticization of the chitosan with water (Despond, Espuche, Cartier, & Domard, 2005). Those water molecules that initially get in the chitosan matrix; may have opened the structure for the water molecule to enter and sorb in the neighborhood of the initially sorbed molecules. This explanation has been given by Starkweather (1980) in the study of water sorption on nylon, and by Zhang, Britt, and Tung (1999) in the case of water on EVOH.

5. Conclusions

Three relaxation processes have been detected in chitosan. At low temperature (243 K) a β-relaxation, with activation energy of 98 kJ mol^{-1} which corresponds to non-cooperative motions. When it is compared with other polysaccharides leads to the conclusion that it corresponds to the rotations of oxocyclic groups such as, –NH_2 or as –$NH^+{}_3{}^-$OOC–CH_3 (quitosonium acetate), –CH_2OH and in some extension –NH–CO–CH_3 of the chitosan. The β-relaxation in the blends, depends on glycerol concentration, it has been interpreted as motions of the side chains of chitosan linked to glycerol by hydrogen bonding At higher temperature two overlapped relaxation processes

α− and α−′. The α-relaxation is susceptible of plasticization with glycerol and it has been attributed to the glass transition of chitosan T_g.

Solid-state NMR has provided a useful tool to study the interaction between glycerol and chitosan in the blends. For high chitosan content, the blends are homogenous and a decrease of the glycerol mobility is observed. As the glycerol concentration is increased, two $T_{1\rho}^{H}$ could be distinguished, corresponding to glycerol and chitosan domains, respectively. These results are in agreement with the assumption of a "*clustering model*" at high glycerol concentrations, consisting of a two-step mechanism. A first step, in which the solvent is sorbed by means of hydrogen bonds on polymer-specific sites such as $–NH_2$or as $–NH^+{}_3{}^-OOC–CH_3$ (quitosonium acetate), $–CH_2OH$ and in some extension $–NH–CO–CH_3$, and a second one, a solvent clustering around the first sorbed solvent molecules forming a hydrogen bonded network of glycerol molecules.

Acknowledgements

This work was financially supported by the Consejo Superior de Investigaciones Científicas (C.S.I.C.). Thanks are also given to the Ministerio de Ciencia y Tecnología for a Project (MAT2005-05648-C02-01) and to the Comunidad Autónoma de Madrid for a Project (CAMS0505/MAT/0227). The authors also thank Aziende Chimica e Farmaceutica (A.C.E.F.) S.p.a. Fiorenzuola D'Arda (Piacenza), Italy, for the kind gift of the chitosan sample. I. Q.-G. gratefully acknowledges financial support from the Ministerio de Ciencia y Tecnología for a Ramón and Cajal contract.

References

Angell, C. A. (1984). In K. L. Ngai & G. B. Wright (Eds.), *Relaxation in complex systems* (p. 3). Washington, DC: Office Naval Research. Naval Research Laboratory.

Arndt, M., Stannarius, R., Gorbatschow, W., & Kremer, F. (1996). Dielectric investigations of the dynamic glass transition in nanopores. *Physical Review E, 54*(5), 5377–5390.

Baker, R. R., Coburn, S., Liu, C., & Tetteh, J. (2005). Pyrolysis of saccharide tobacco ingredients: a TGA-FTIR investigation. *Journal of Analytical and Applied Pyrolysis, 74*(1–2), 171–180.

Barrales-Rienda, J. M., & Pepper, D. C. (1966). Intrinsic viscosities and dimensions of poly (phenylene oxide). *Journal of Polymer Science Part B: Polymer Letters, 4*, 939–941.

Berth, G., Dautzenberg, H., & Peter, M. G. (1998). Physico-chemical characterization of chitosans varying in degree of acetylation. *Carbohydrate Polymers, 36*(2–3), 205–216.

Biliaderis, C. G., Lazaridou, A., & Arvanitoyannis, I. (1999). Glass transition and physical properties of polyol-plasticised pullulan-starch blends at low moisture. *Carbohydrate Polymers, 40*(1), 29–47.

Bohdanecký, M., & Kovár, J. (1982). Viscosity of polymer solutions. In A. D. Jenkins (Ed.), *Polymer Science Library* (pp. 87–88). Amsterdam: Elsevier.

Böhmer, R., & Hinze, G. (1998). Reorientations in supercooled glycerol studied by two-dimensional time-domain deuteron nuclear magnetic resonance spectroscopy. *Journal of Chemical Physics, 109*(1), 241–248.

Brown, C. D., Kreilgaard, L., Nakakura, M., Caram-Lelham, N., Pettit, D. K., Gombotz, W. R., et al. (2001). Release of pegylated granulocyte–macrophage colony-stimulating factor from chitosan/glycerol films. *Journal of Controlled Release, 72*(1–3), 35–46.

Cardenas, G., & Miranda, S. P. (2004). FTIR and TGA studies of chitosan composite films. *Journal of the Chilean Chemical Society, 49*(4), 291–295.

Cervera, M. F., Heinamaki, J., Rasanen, M., Maunu, S. L., Karjalainen, M., Acosta, O. M. N., et al. (2004). Solid-state characterization of chitosans derived from lobster chitin. *Carbohydrate Polymers, 58*(4), 401–408.

Chan, R. K., Pathmanathan, K., & Johari, G. P. (1986). Dielectric relaxations in the liquid and glassy states of glucose and its water mixtures. *Journal of Physical Chemistry, 90*(23), 6358–6362.

Cheung, M. K., Wan, K. P. Y., & Yu, P. H. (2002). Miscibility and morphology of chiral semicrystalline poly-(R)-(3-hydroxybutyrate)/chitosan and poly-(R)-(3-hydroxybutyrate-co-3-hydroxyvalerate)/chitosan blends studied with DSC, ^1H T_1 and $T_1\rho$ CRAMPS. *Journal of Applied Polymer Science, 86*(5), 1253–1258.

Despond, S., Espuche, E., Cartier, N., & Domard, A. (2005). Hydration mechanism of polysaccharides: a comparative study. *Journal of Polymer Science Part B-Polymer Physics, 43*(1), 48–58.

Dong, Y. M., Ruan, Y. H., Wang, H. W., Zhao, Y. G., & Bi, D. X. (2004). Studies on glass transition temperature of chitosan with four techniques. *Journal of Applied Polymer Science, 93*(4), 1553–1558.

Economy, J., Storm, R. S., Matkovich, V. I., Cottis, S. G., & Nowak, B. E. (1976). Synthesis and structure of para-hydroxybenzoic acid polymer. *Journal of Polymer Science Part A: Polymer Chemistry, 14*(9), 2207–2224.

Einfeldt, J., Meißner, D., & Kwasniewski, A. (2001). Polymer dynamics of cellulose and other polysaccharides in solid state-secondary dielectric relaxation processes. *Progress in Polymer Science, 26*(9), 1419–1472.

Einfeldt, J., Meißner, D., & Kwasniewski, A. (2003). Contributions to the molecular origin of the dielectric relaxation processes in polysaccharides – the high temperature range. *Journal of Non-Crystalline Solids, 320*(1–3), 40–55.

Einfeldt, J., Meißner, D., & Kwasniewski, A. (2004). Molecular interpretation of the main relaxations found in dielectric spectra of cellulose – experimental arguments. *Cellulose, 11*(2), 137–150.

Enns, J. B., & Simha, R. (1977). Transitions in semicrystalline polymers. 2. polyoxymethylene and poly(ethylene oxide). *Journal Macromolecular Science – Physics, B13*(1), 25–47.

Erman, B., Flory, P. J., & Hummel, J. P. (1980). Moments of the end-to-end vectors for para-phenylene polyamides and polyesters. *Macromolecules, 13*(3), 484–491.

Fuoss, R. F. (1941). Electrical properties of solids .VII. The system polyvinyl chloride-diphenyl. *Journal of the American Chemical Society, 63*, 378–385.

Genta, I., Pavanetto, F., Conti, B., Giunchedi, P., & Conte, U. (1995). Improvement of dexamethasone dissolution rate from spray-dried chitosan microspheres. *STP Pharma Sciences, 5*(3), 202–207.

Gillham, J. K., Benci, J. A., & Boyer, R. F. (1976). Investigation of T_{11} (greater than T_g) transition in polystyrene by torsional braid analysis. *Polymer Engineering Science, 16*(5), 357–360.

Gordon, M., & Taylor, J. S. (1952). Ideal copolymers and the 2nd-order transitions of synthetic rubbers. 1. Non-crystalline copolymers. *Journal of Applied Chemistry, 2*(9), 493–500.

Götze, W., & Sjögren, L. (1992). Relaxation processes in supercooled liquids. *Reports on Progress in Physics, 55*(3), 241–376.

Guan, Y. L., Liu, X. F., Zhang, Y. P., & Yao, K. D. (1998). Study of phase behavior on chitosan/viscose rayon blend film. *Journal of Applied Polymer Science, 67*(12), 1965–1972.

Hansen, C., & Richert, R. (1997). Dipolar dynamics of low-molecular-weight organic materials in the glassy state. *Journal of Physics-Condensed Matter, 9*(44), 9661–9671.

Hummel, J. P., & Flory, P. J. (1980). Structural geometry and torsional potentials in para-phenylene polyamides and polyesters. *Macromolecules, 13*(3), 479–484.

Ikejima, T., & Inoue, Y. (2000). Crystallization behavior and environmental biodegradability of the blend films of poly(3-hydroxybutyric acid) with chitin and chitosan. *Carbohydrate Polymers, 41*(4), 351–356.

Jacoby, P., Bersted, B. H., Kissel, W. J., & Smith, C. E. (1986). Studies on the β-crystalline form of isotactic polypropylene. *Journal Polymer SciencePart B: Polymer Physics, 24*(3), 461–491.

Kalichevsky, M. T., Jaroszkiewicz, E. M., Ablett, S., Blanshard, J. M. V., & Lillford, P. J. (1992). The glass-transition of amylopectin measured by DSC, DMTA and NMR. *Carbohydrate Polymers, 18*(2), 77–88.

Kalichevsky, M. T., Jaroszkiewicz, E. M., & Blanshard, J. M. V. (1992). Glass-transition of gluten. 1. Gluten and gluten sugar mixtures. *International Journal of Biological Macromolecules, 14*(5), 257–266.

Kaymin, I. F., Ozolinya, G. A., & Plisko, E. A. (1980). Investigation of temperature transitions of chitosan. *Polymer Science USSR, 22*(1), 151–156.

Kelley, S. S., Rials, T. G., & Glasser, W. G. (1987). Relaxation behavior of the amorphous components of wood. *Journal of Materials Science, 22*(2), 617–624.

Kerwin, J. L., Whitney, D. L., & Sheikh, A. (1999). Mass spectrometric profiling of glucosamine, glucosamine polymers and their catecholamine adducts – model reactions and cuticular hydrolysates of toxorhynchites amboinensis (culicidae) pupae. *Insect Biochemistry and Molecular Biology, 29*(7), 599–607.

Knaul, J. Z., Kasaai, M. R., Bui, V. T., & Creber, K. A. M. (1998). Characterization of deacetylated chitosan and chitosan molecular weight review. *Canadian Journal of Chemistry, 76*(11), 1699–1706.

Kruiskamp, P. H., Smits, A. L. M., Van Soest, J. J. G., & Vliegenthart, J. F. G. (2001). The influence of plasticiser on molecular organization in dry amylopectin measured by differential scanning calorimetry and solid state nuclear magnetic resonance spectroscopy. *Journal of Industrial Microbiology and Biotechnology, 26*(1–2), 90–93.

Korus, J., Hempel, E., Beiner, M., Kahle, S., & Donth, E. (1997). Temperature dependence of α glass transition cooperativity. *Acta Polymerica, 48*(9), 369–378.

Lavertu, M., Xia, Z., Serreqi, A. N., Berrada, M., Rodrigues, A., Wang, D., et al. (2003). A validated ^{1}H NMR method for the determination of the degree of deacetylation of chitosan. *Journal of Pharmaceutical and Biomedical Analysis, 32*(6), 1149–1158.

Lazaridou, A., & Biliaderis, C. G. (2002). Thermophysical properties of chitosan, chitosan-starch and chitosan-pullulan films near the glass transition. *Carbohydrate Polymers, 48*(2), 179–190.

LeMeste, M., Roudaut, G., & Davidou, S. (1996). Thermomechanical properties of glassy cereal foods. *Journal of Thermal Analysis, 47*(5), 1361–1375.

Lourdin, D., Coignard, L., Bizot, H., & Colonna, P. (1997). Influence of equilibrium relative humidity and plasticizer concentration on the water content and glass transition of starch materials. *Polymer, 38*(31), 5401–5406.

Lourdin, D., Bizot, H., & Collonna, P. (1997). Antiplastization in starch–glycerol films?. *Journal Applied Polymer Science 63*(8), 1047–1053.

Lourdin, D., Ring, S. G., & Colonna, P. (1998). Study of plasycizer-oligomer and plasticizer-polymer interactions by dielectric analysis: maltose–glycerol and amylose–glycerol.water systems. *Carbohydrate Research, 306*(4), 551–558.

Lourdin, D., Colonnna, P., & Ring, S. G. (2003). Volumetric behaviour of maltose–water, maltose–glycerol and starch–sorbitol–water systems mixtures in relation to structural relaxations. *Carbohydrate Research, 338*(24), 2883–2887.

MacInnes, W. M. (1993). In J. M. V. Blanshard & P. J. Lillford (Eds.), *The glassy state in foods* (pp. 223–248). Nottingham: UK Nottingham University Press.

Masciovecchio, C., Monaco, G., Ruocco, G., Sette, F., Cunsolo, A., Krisch, M., et al. (1998). High frequency dynamics of glass forming liquids at the glass transition. *Physical Review Letters, 80*(3), 544–547.

Mathew, A. P., & Dufresne, A. (2002). Plasticized waxy maize starch: effect of polyols and relative humidity on material properties. *Biomacromolecules, 3*(5), 1101–1108.

Meißner, D., Einfeldt, J., & Kwasniewski, A. (2000). Contributions to the molecular origin of the dielectric relaxation processes in polysaccharides – the low temperature range. *Journal of Non-Crystalline Solids, 275*(3), 199–209.

Meißner, D., Einfeldt, L., & Einfeldt, J. (2001). Dielectric relaxation analysis of cellulose oligomers and polymers in dependency on their chain length. *Journal of Polymer Science Part B: Polymer Physics, 39*(20), 2491–2500.

Montès, H., Cavaillé, J. Y., & Mazeau, K. (1994). Secondary relaxations in amorphous cellulose. *Journal of Non-Crystalline Solids, 172*, 990–995.

Moore, W. R. (1967). *Viscosities of dilute polymer solutions. Progress in Polymer Science*. Oxford: Pergamon Press, pp. 3–43.

Murphy, E. J. (1962). Thermal decomposition of natural cellulose in vacuo. *Journal of Polymer Science, 58*(166), 649–655.

Ogura, K., Kanamoto, T., Itoh, M., Miyashiro, H., & Tanaka, K. (1980). Dynamic mechanical-behavior of chitin and chitosan. *Polymer Bulletin, 2*(5), 301–304.

Pappa, A., Mikedi, K., Tzamtzis, N., & Statheropoulos, M. (2003). Chemometric methods for studying the effects of chemicals on cellulose pyrolysis by thermogravimetry-mass spectrometry. *Journal of Analytical and Applied Pyrolysis, 67*(2), 221–235.

Partanen, R., Marie, V., MacNaughtan, W., Forssell, P., & Farhat, I. (2004). ^{1}H NMR study of amylose films plasticised by glycerol and water. *Carbohydrate Polymers, 56*(2), 147–155.

Pizzoli, M., Ceccorulli, G., & Scandola, M. (1991). Molecular motions of chitosan in the solid-state. *Carbohydrate Research, 222*, 205–213.

Portero, A., Remunan-López, C., & Vila-Jato, J. L. (1998). Effect of chitosan and chitosan glutamate enhancing the dissolution properties of the poorly water soluble drug nifedipine. *International Journal of Pharmaceutics, 175*(1), 75–84.

Quijada-Garrido, I., Barrales-Rienda, J. M., Pereña, J. M., & Frutos, G. (1997). Dynamic mechanical and dielectric behavior of erucamide (13-cis-docosenamide), isotactic poly(propylene), and their blends. *Journal of Polymer Science Part B: Polymer Physics, 35*(10), 1473–1482.

Quijada-Garrido, I., Wilhelm, M., Spiess, H. W., & Barrales-Rienda, J. M. (1998). Solid-state NMR studies of structure and dynamics of erucamide isotactic poly(propylene) blends. *Macromolecular Chemistry and Physics, 199*(6), 985–995.

Radloff, D., Boeffel, C., & Spiess, H. W. (1996). Cellulose and cellulose poly(vinyl alcohol) blends .2. Water organization revealed by solid-state NMR spectroscopy. *Macromolecules, 29*(5), 1528–1534.

Ratto, J. A., Chen, C. C., & Blumstein, R. B. (1996). Phase behavior study of chitosan/polyamide blends. *Journal of Applied Polymer Science, 59*(9), 1451–1461.

Ravi Kumar, M. N. V. (1999). Chitin and chitosan fibres: A review. *Bulletin of Materials Science, 22*(5), 905–915.

Ravi Kumar, M. N. V. (2000). A review of chitin and chitosan applications. *Reactive and Functional Polymers, 46*, 1–27.

Reinsberg, S. A., Qiu, X. H., Wilhelm, M., Spiess, H. W., & Ediger, M. D. (2001). Length scale of dynamic heterogeneity in supercooled glycerol near T_g. *Journal of Chemical Physics, 114*(17), 7299–7302.

Romero Colomer, F. R., Meseguer Dueñas, J. M., Gomez Ribelles, J. L., Barrales-Rienda, J. M., & Bautista Ojeda, J. M. (1993). Side-chain liquid-crystalline poly(*N*-maleimides). 5. Dielectric-relaxation behavior of liquid-crystalline side-chain and amorphous poly(*N*-maleimides) – a comparative structural study. *Macromolecules, 26*(1), 155–166.

Rotter, G., & Ishida, H. (1992). Dynamic mechanical analysis of the glass transition: curve resolving applied to polymer. *Macromolecules, 25*(8), 2170–2176.

Ryabov, Y. E., Hayashi, Y., Gutina, A., & Feldman, Y. (2003). Features of supercooled glycerol dynamics. *Physical Review B, 67*(13), 132202/1–132202/4.

Sakurai, K., Maegawa, T., & Takahashi, T. (2000). Glass transition temperature of chitosan and miscibility of chitosan/poly(n-vinyl pyrrolidone) blends. *Polymer, 41*(19), 7051–7056.

Schiener, B., Chamberlin, R. V., Diezemann, G., & Böhmer, R. (1997). Nonresonant dielectric hole burning spectroscopy of supercooled liquids. *Journal of Chemical Physics, 107*(19), 7746–7761.

Shahidi, F., Arachchi, J. K. V., & Jeon, Y. J. (1999). Food applications of chitin and chitosans. *Trends in Food Science and Technology, 10*(2), 37–51.

Shantha, K. L., & Harding, D. R. K. (2002). Synthesis and characterisation of chemically modified chitosan microspheres. *Carbohydrate Polymers, 48*(3), 247–253.

Simatos, D., Blond, G., & Perez, J. (1995). In V. Barbosa-Canovas & L. Welti-Chanes (Eds.), *Food preservation by moisture control* (pp. 3–31). Lancaster, PA: Technomic Publishing.

Singh, D. K., & Ray, A. R. (1998). Characterization of grafted chitosan films. *Carbohydrate Polymers, 36*(2-s), 251–255.

Smits, A. L. M., Hulleman, S. H. D., Van Soest, J. J. G., Feil, H., & Vliegenthart, F. G. (1999). The influence of polyols on the molecular organization in starch-based plastics. *Polymers for Advanced Technologies, 10*(10), 570–573.

Smits, A. L. M., Kruiskamp, P. H., VanSoest, J. J. G., & Vliegenthart, J. F. G. (2003). Interaction between dry starch and plasticisers glycerol or ethylene glycol, measured by differential scanning calorimetry and solid state NMR spectroscopy. *Carbohydrate Polymers, 53*(4), 409–416.

Sokolov, A. P., Kisliuk, A., Quitmann, D., Kudlik, A., & Rössler, E. (1994). The dynamics of strong and fragile glass formers – vibrational and relaxation contributions. *Journal of Non-Crystalline Solids, 172*, 138–153.

Sokolov, A. P., Steffen, W., & Rössler, E. (1995). High-temperature dynamics in glass-forming liquids. *Physical Review E, 52*(5), 5105–5109.

Sperling, L. H. (1986). *Introduction to physical polymer science*. New York: Wiley.

Starkweather, H. M. (1980). In S. P. Rowland (Ed.), *Water in polymers* (pp. 433). Washington, DC: American Chemical Society.

Struszczyk, H. (1987). Microcrystalline chitosan. I. Preparation and properties of microcrystalline chitosan. *Journal of Applied Polymer Science, 33*(1), 177–189.

Suyatma, N. E., Tighzert, L., & Copinet, A. (2005). Effects of hydrophilic plasticizers on mechanical, thermal, and surface properties of chitosan films. *Journal of Agricultural and Food Chemistry, 53*(10), 3950–3957.

Tanabe, T., Okitsu, N., Tachibana, A., & Yamauchi, K. (2002). Preparation and characterization of keratin–chitosan composite film. *Biomaterials, 23*(3), 817–825.

Thomazine, M., Carvalho, R. A., & Sobral, P. I. A. (2005). Physical properties of gelatin films plasticized by blends of glycerol and sorbitol. *Journal of Food Science, 70*(3), E172–E176.

Toffey, A., Samaranayake, G., Frazier, C. E., & Glasser, W. G. (1996). Chitin derivatives. I. Kinetics of the heat-induced conversion of chitosan to chitin. *Journal of Applied Polymer Science, 60*(1), 75–85.

Toffey, A., & Glasser, W. G. (2001). Chitin derivatives III Formation of amidized homologs of chitosan. *Cellulose, 8*(1), 35–47.

Viciosa, M. T., Dionisio, M., Silva, R. M., Reis, R. L., & Mano, J. F. (2004). Molecular motions in chitosan studied by dielectric relaxation spectroscopy. *Biomacromolecules, 5*(5), 2073–2078.

Viciosa, M. T., Dionisio, M., & Mano, J. F. (2006). Dielectric characterization of neutralized and nonneutralized chitosan upon drying. *Biopolymers, 81*(3), 149–159.

Wanjun, T., Cunxin, W., & Donghua, C. (2005). Kinetic studies on the pyrolysis of chitin and chitosan. *Polymer Degradation and Stability, 87*(3), 389–394.

Wood, L. A. (1958). Glass transition temperatures of copolymers. *Journal of Polymer Science, 28*(117), 319–330.

Wu, C., Yamagishi, T., Nakamoto, Y., Ishida, S., Nitta, K., & Kubota, S. (2000). Organic hybrid of chlorinated polyethylene and hindered phenol. I. Dynamic mechanical properties. *Journal of Polymer Science Part B: Polymer Physics, 38*(17), 2285–2295.

Wu, C., Zhou, S. Q., & Wang, W. (1995). A dynamic laser light-scattering study of chitosan in aqueous-solution. *Biopolymers, 35*(4), 385–392.

Wu, C. F. (2001). A novel second-order transition in organic hybrids consisting of polymers and small molecules. *Chinese Journal of Polymer Science, 19*(5), 455–466.

Xiao, C. B., Zhang, Z. J., Zhang, J. H., Lu, Y. S., & Zhang, L. (2003). Properties of regenerated cellulose films plasticized with alpha-monoglycerides. *Journal of Applied Polymer Science, 89*(13), 3500–3505.

Zhang, X. Q., Burgar, I., Do, M. D., & Lourbakos, E. (2005). Intermolecular interactions and phase structures of plasticized wheat proteins materials. *Biomacromolecules, 6*(3), 1661–1671.

Zhang, X. Q., Burgar, I., Lourbakos, E., & Beh, H. (2004). The mechanical property and phase structures of wheat proteins/polyvinyl alcohol blends studied by high-resolution solid-state NMR. *Polymer, 45*(10), 3305–3312.

Zhang, Z. B., Britt, I. J., & Tung, M. A. (1999). Water absorption in EVOH films and its influence on glass transition temperature. *Journal of Polymer Science Part B-Polymer Physics, 37*(7), 691–699.

Zohuriaan, M. J., & Shokrolahi, F. (2004). Thermal studies on natural and modified gums. *Polymer Testing, 23*(5), 575–579.

Zong, Z., Kimura, Y., Takahashi, M., & Yamane, H. (2000). Characterization of chemical and solid state structures of acylated chitosans. *Polymer, 41*(3), 899–906.